scientific reports

OPEN

Spatiotemporal aberrations due to the groove density mismatching of compression gratings in ultra-intense femtosecond lasers

Yang Zhao[1,2,3], Fenxiang Wu[2,3], Cheng Wang[2], Jiabing Hu[2], Zongxin Zhang[2], Xingyan Liu[2], Xiaojun Yang[2], Peile Bai[2], Haidong Chen[2], Jiayi Qian[2], Jiayan Gui[2], Yi Xu[2✉], Yuxin Leng[2✉] & Ruxin Li[2✉]

The groove density mismatching of compression gratings, an often-neglected key issue, can induce significant spatiotemporal aberrations especially for super-intense femtosecond lasers. We mainly investigate the angular chirp and the consequent degradation of the effective focused intensity introduced by the groove density mismatching of compression gratings in ultra-intense femtosecond lasers. The results indicate that the tolerances of grating groove density mismatching will rapidly decrease with the beam aperture or spectral bandwidth increases. For our 100PW laser under construction, the grating groove density mismatching should be as small as 0.001 gr/mm if the drop of effective focused intensity has to be controlled below 15%. More importantly, new angular chirp compensation schemes are proposed for both double-grating and four-grating compressors. This work reveals the importance of groove density matching of compression gratings, and can provide helpful guidelines for the design of ultra-intense femtosecond lasers.

The ultra-intense femtosecond lasers play an important role in strong field sciences, as they can create extreme conditions and offer unprecedented means for the frontier physical research. Profiting from the chirped pulse amplification (CPA) and the optical parametric chirped pulse amplification (OPCPA) technologies[1,2], the peak power of femtosecond lasers rapidly increases. At present, the hundreds-of-terawatts (TW) and petawatt (PW) class femtosecond lasers have been built around the world, and the corresponding focused intensity has reached up to $10^{22} \sim 10^{23}$ W/cm^2[3–10]. Besides, the 10PW class femtosecond lasers, such as SULF-10PW in China, ELI-10PW in Romania and L4 Aton at ELI beamlines in the Czech Republic have also been successfully developed[11–14]. This is the currently realized highest laser peak power. What is more, to pursue higher peak power and focused intensity, tens-of-PW or 100PW laser systems have already been proposed and under construction, including the OPAL-75PW in USA, the SEL-100PW in China, the XCELS-200PW in Russia, and the ELI-200PW in Europe[15–19].

As the final stage among the stretching-amplification-compression chain of CPA and OPCPA systems, the laser compressor composed of parallel grating pairs plays a crucial role in realizing ultra-intense laser pulses. On one hand, appropriate dispersion should be introduced to obtain near Fourier-transfer-limit (FTL) laser pulses, which has been well studied[20–22]. On the other hand, the compression gratings matching becomes increasingly important, as spectral bandwidth and beam aperture increase. Indeed, a slight mismatching of compression gratings will induce residual angular chirp[23–25], which can distort the spatiotemporal shape of laser pulses and finally reduce the effective focused intensity. Angular chirp usually originates from the misalignment of the compression gratings, which leads to the tilted pulse front. As a result, the focal spot is enlarged and the pulse duration is stretched[26]. For wavefront errors induced by the gratings, due to the separation and superposition of various spectral components in space, spatio-spectral phase coupling is caused, which leads to more complex spatiotemporal coupling distortion in the output pulse[27,28]. In fact, in ultra-intense femtosecond lasers, the compressor is set up in a vacuum environment, and the local heating introduced by the laser will cause a surface deformation of the gratings easily, and then the high order spatiotemporal coupling appears[29]. To sum up, since high peak power lasers usually feature with broadband spectrum and large beam aperture, the impact

[1]School of Physics Science and Engineering, Tongji University, Shanghai 200092, China. [2]State Key Laboratory of High Field Laser Physics and CAS Center for Excellence in Ultra-Intense Laser Science, Shanghai Institute of Optics and Fine Mechanics, Chinese Academy of Sciences, Shanghai 201800, China. [3]These authors contributed equally: Yang Zhao and Fenxiang Wu. ✉email: xuyi@siom.ac.cn; lengyuxin@mail.siom.ac.cn; ruxinli@siom.ac.cn

of compression gratings mismatching is serious. Unfortunately, the needed size of compression gratings in high peak power lasers are generally large to avoid optical damage. For example, the meter-sized gratings are required for 10PW laser compression. However, the perfect matching of such large-size gratings is particularly difficult.

The compression gratings mismatching mainly includes the grating pair misalignment and the grating groove density mismatching. Both of them can result in spatiotemporal aberrations and hence significant effective intensity degradation in the far field, especially for ultra-intense femtosecond lasers. The impact of grating pair misalignment has been comprehensively investigated[23–26,30–32], and the guidance of the grating calibration accuracy in three dimensions are proposed in our previous work[32]. However, there are seldom attentions paid to the grating groove density mismatching in laser compressor. Usually, limited by the grating manufacturing technology, gratings produced in different batches cannot guarantee identical groove density, which leads to inter-grating groove density mismatching. Currently, most of the works about grating groove density are focused on its measurement, and some measurement methods have been developed. Such as the Atomic Force Microscopy[33,34], the Long Trace Profile[35–37] and the diffraction method[38–42]. The measurement accuracy of inter-grating groove density error can reach 0.005 gr/mm[43]. Nevertheless, this groove density error (0.005 gr/mm) may no longer be sufficient for future tens-of-PW and 100PW class lasers, because a tiny grating groove density mismatching in compressors can induce serious spatiotemporal aberrations of ultra-intense femtosecond lasers. Previously, to eliminate the angular chirp induced by grating pair misalignment, researchers have put forward that two types of errors with similar effects can be balanced against each other[24,44,45]. For example, we can adjust the grating tip to counteract the vertical angular chirp introduced by groove non-parallelism. For the complex spatiotemporal coupling distortion induced by the imperfect diffraction wave-front of gratings, Li et al. insert a scaled down compressor with a deformable retro-reflection mirror before the main compressor[46]. The wave-front generated by the deformable mirror can compensate that introduced by the second and the third gratings in the main compressor, and then spatiotemporal coupling distortion can be perfectly removed. The similar method has also been used to suppress the effect caused by grating groove density mismatching[47]. Although people successfully corrected the offset angle of output laser beam, the residual angular chirp is significantly increased and hence the effective focused intensity is further decreased. However, this problem has not been taken seriously as yet. Therefore, it is of great importance and an urgent need to propose a more efficient compensation method for the grating groove density mismatching in ultra-intense femtosecond lasers.

In this work, the angular chirp and the consequent effective intensity degradation induced by groove density mismatching of compression gratings are investigated, which is an important but often ignored issue in ultra-intense femtosecond lasers. The results show that the degradation of effective focused intensity induced by grating groove density mismatching will aggravate with the increase of spectral bandwidth or beam aperture. Some typical high peak power femtosecond lasers are applied as case studies, and the tolerances of groove density mismatching of compression gratings are discussed. For our 100PW laser being built now[17], the tolerance of grating groove density mismatching is only 0.001 gr/mm for an effective intensity drop below 15%. It is a serious challenge for current gratings manufacturing and testing techniques. Hence, some efficient compensation methods for the grating groove density mismatching are needed. For the double-grating compressors, a new compensation scheme based on the suppression of the angular chirp rather than the offset angle is proposed. And this scheme is demonstrated to be much more favorable for controlling the effective intensity degradation. Moreover, we also proposed a two-step compensation method for the angular chirp of the output pulses from four-grating compressors. Particularly, for the compressor happens to be the mirror-symmetry configuration of a double-grating compressor, the angular chirp can be cancelled out just by optimizing the collocation of grating pairs. This work efficiently demonstrates the importance of groove density matching of compression gratings, and can promote the developments of grating technologies and ultra-intense femtosecond lasers.

Angular chirp caused by the grating groove density mismatching in compressors

In order to obtain high spatial–temporal quality pulses from a high peak power femtosecond laser, it is necessary to ensure the perfect alignment of compression gratings. Several studies have proved that the compression gratings misalignment in any dimension can induce angular chirp, which ultimately affects the spatiotemporal characteristic of laser pulses[23–25,30–32]. Analogously, if there is an error of the grating groove density in a compressor, the angular chirp will also be introduced even the gratings are aligned precisely.

Firstly, a double-grating compressor is investigated based on the grating diffraction equation and ray-tracing method, as shown in Fig. 1. The red and black rays represent the propagation optical paths of laser pulses in this compressor with and without groove density mismatching. The groove densities of G1 and G2 are N and N', respectively. In the case of N'=N, the incident laser ray firstly passes through OB and BC, then returns by its original path after being reflected at point C, and finally emits from point O. However, due to the presence of groove density error (i.e. N'≠N), the laser ray will deviate from its initial propagation direction after being diffracted by G2 for the first time. The deviated laser ray is reflected at point C', then passes through C'D and DE, and finally outputs from point E. Consequently, an offset angle θ_d is induced between the incident and output laser rays. Generally, the groove density error is very tiny, hence θ_d is also very small and can be expressed as Eq. (1). ΔN_d is the grating groove density error of a double-grating compressor, λ is the wavelength of laser ray, and α is the laser incident angle on G1. Here, we only exhibit the beam trajectory for a single wavelength, but it can be applied to the entire spectrum of the laser pulses.

$$\theta_d = 2\delta = \frac{2(N\prime - N) \cdot \lambda}{cos\alpha} = \frac{2\Delta N_d \cdot \lambda}{cos\alpha}. \tag{1}$$

Obviously, the offset angle θ_d of the output laser ray is wavelength dependent. In other words, an angular chirp is introduced to the output laser beam. It is notable that the laser ray is always propagating within the diffraction
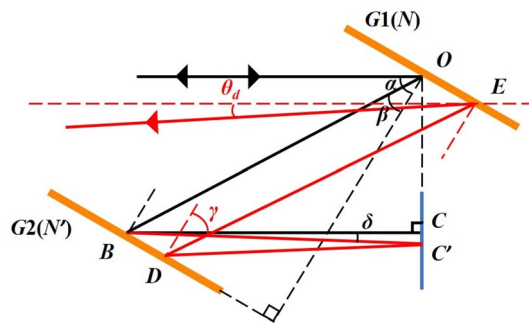
Figure 1. Schematic of groove density mismatching in a double-grating compressor.

plane of gratings, and there are no additional components perpendicular to the diffraction plane. Therefore, the grating groove density mismatching only causes an angular chirp in the horizontal direction, and the angular chirp can be given as Eq. (2).

$$C_{ad} = \frac{d\theta_d}{d\lambda} = 2 \cdot \frac{\Delta N_d}{cos\alpha}. \tag{2}$$

Secondly, the four-grating compressors which are more commonly used in ultra-intense femtosecond lasers are also investigated. As Fig. 2 shows, the groove densities of the four gratings are $N1$, $N2$, $N3$ and $N4$, respectively. Based on the grating diffraction equation and ray-tracing method, we can also obtain the offset angle θ_f of the output laser rays from above four-grating compressor, as Eq. (3).

$$\theta_f = \frac{[(N2 + N3) - (N1 + N4)] \cdot \lambda}{cos\alpha}. \tag{3}$$

$$C_{af} = \frac{d\theta_f}{d\lambda} = \frac{(N2 + N3) - (N1 + N4)}{cos\alpha} \tag{4}$$

$$\Delta N_f = \frac{(N2 + N3) - (N1 + N4)}{2} \tag{5}$$

Then the corresponding angular chirp C_{af} of output laser rays can be calculated by Eq. (4). Here, we can define the groove density error ΔN_f of a four-grating compressor as Eq. (5), which is also applicable for a double-grating compressor. Because the configuration of a double-grating compressor is equivalent to a mirror-symmetry grating pair, which means $N2 = N3 = N'$ and $N1 = N4 = N$. As a result, $\Delta N = \Delta N_d = \Delta N_f$.

Given above, we find that the grating groove density mismatching in compressors will induce angular chirp of output laser pulses. But it is worth noting that the angular chirp is a constant, which only depends on the laser incident angle and the grating groove density error ΔN. In the subsequent chapters, the spatiotemporal aberrations due to the groove density mismatching of compression gratings in ultra-intense femtosecond lasers will be analyzed.

Spatiotemporal aberrations induced by grating groove density mismatching

The angular chirp induced by the grating groove density mismatching can destruct the spatiotemporal characteristics of the laser beam and ultimately degrade the effective focused intensity, especially for ultra-intense femtosecond lasers. Due to the presence of angular chirp, each spectral component of the angular chirped laser pulses will have a spatial displacement at the focal spot, which causes spectral narrowing and hence the local pulse duration elongation at each point inside the focal region. In the time domain, the angular chirp will also induce pulse front tilt, which can generate a group delay on the cross section of laser beam. As a result, the pulses at different radial positions of laser beam arrive at the focal plane at different time. In other words, the focal
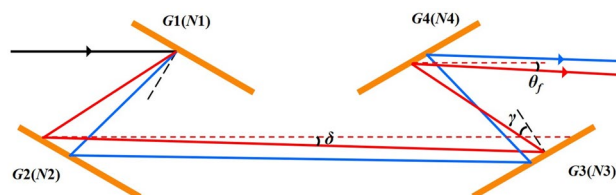

Figure 2. Schematic of groove density mismatching in a four-grating compressor.

plane is not illuminated simultaneously, i.e., the effective pulse duration at focal region is much longer than the local pulse duration. In addition to the spectral decomposition, the angular chirp will also increase the beam divergence of compressed pulses and finally result in focal spot size enlargement in the direction of angular chirp. The expansion factors of local pulse duration and focal spot size are almost the same. In our previous work, the three main far-field effects aforesaid of angular chirp, i.e., the local pulse duration (τ_l) elongation, the effective pulse duration (τ_e) broadening, and the focal spot size enlargement, have been comprehensive investigated.

Similarly, the groove density mismatching of compression gratings induced angular chirp will also result in pulse duration elongation, effective pulse duration broadening and focal spot size enlargement in the far field, and hence degrade the effective focused intensity. Based on the calculation method in Reference[32], the far-field effects of the groove density mismatching of compression gratings are numerically analyzed with different spectral bandwidth and beam aperture, shown as Fig. 3. In the calculations, for the sake of simplicity, the laser pulses are assumed to feature with Gaussian spectra centered at 800 nm wavelength and uniform spatial intensity distribution. The incident angle and standard grating groove density of the grating compressor are 51° and 1480 gr/mm, respectively. τ_0 is the FTL pulse duration, d_0 is the ideal focal spot diameter while d represents focal spot diameter in the direction of angular chirp. I_0 is ideal focused intensity.

In the first case, the pulse spectral bandwidth is 100 nm, and the beam aperture is changing from 50 to 400 mm. The elongation of the far field local pulse duration, the broadening of the effective pulse duration, and the enlargement of the focal spot size are calculated with different grating groove density errors. As shown in Fig. 3a–c, as the grating groove density error increases, the far field local pulse duration, the effective pulse duration and the focal spot size are all increasing, which ultimately leads to focused intensity degradation shown in Fig. 3d. Moreover, it is obvious that the laser with larger beam aperture has longer pulse duration and more significant focal spot enlargement, and hence the lower focused intensity, for a certain grating groove density error. It means that the larger-aperture lasers have smaller tolerances to the grating groove density mismatching.

In the second case, the grating groove density error induced spatiotemporal aberrations of laser pulses are calculated with different spectral bandwidth, while the beam aperture is 200 mm. As Fig. 3e–g show, the variation trends of far field local pulse duration, the effective pulse duration and the focal spot size are the same as Fig. 3a–c, with the grating groove density error increases. Therefore, the focused intensity degradation in Fig. 3h follow the same trend as Fig. 3d. As well, for the same grating groove density error, the lasers with wider spectra have more significant spatiotemporal aberrations and are more sensitive to the grating groove density mismatching.

In a word, for ultra-intense femtosecond lasers that usually feature with large beam aperture and broad spectral bandwidth, even tiny grating groove density mismatching can result in significant distortions of laser spatiotemporal characteristics and consequently a serious degradation of the focused intensity. What's more, with the development of ultra-intense femtosecond lasers, the grating groove density mismatching will be of crucial importance to the effective focused intensity. Thereby, investigating the influence of grating groove density mismatching in compressor and proposing effective compensation methods are necessary and significant for obtaining ideal ultra-intense laser pulses.

A new compensation scheme for double-grating compressors

The double-grating compressors are generally employed in hundreds-of-TW lasers. In this section, a CPA-based 200TW femtosecond laser in our laboratory will be numerically investigated[3], including the influence and compensation of the grating groove density mismatching in compressor.
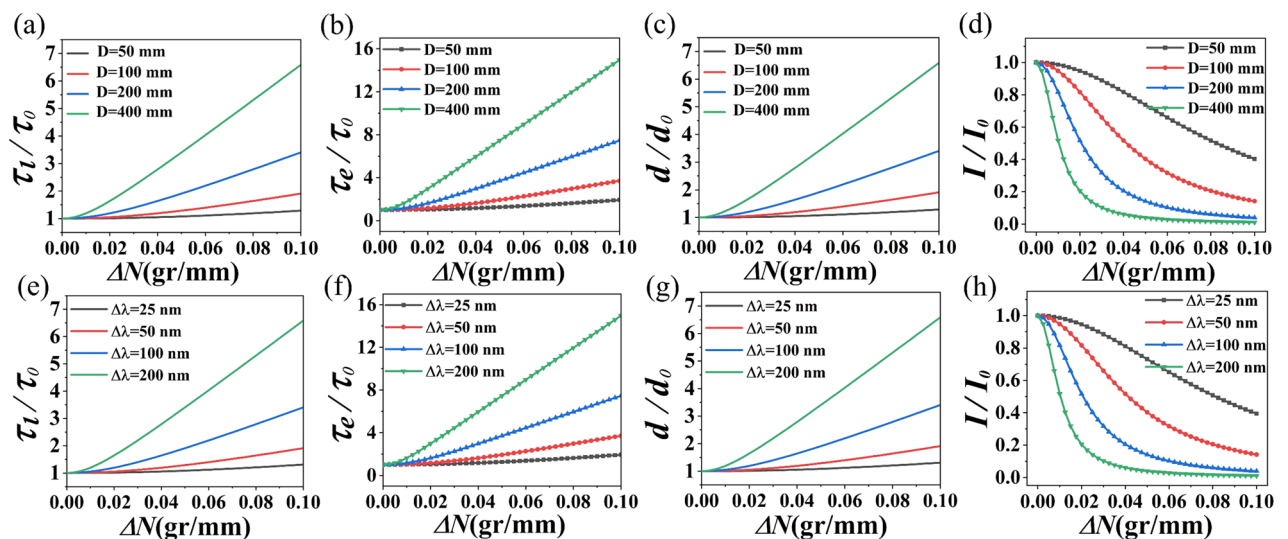

Figure 3. Local pulse duration elongation factor (**a**,**e**), effective pulse duration broadening factor (**b**,**f**), focal spot size enlargement factor (**c**,**g**) and effective intensity degradation (**d**,**h**), with the increase of grating groove density error. (**a**–**d**): different beam apertures with 100 nm spectral bandwidth; (**e**–**h**): different spectral bandwidths with 200 mm beam aperture.

For the sake of simplicity, the laser is described by a Gaussian spectrum with 800 nm center wavelength and 90 nm bandwidth (at $1/e^2$), and the compressed pulse duration is around 27 fs. The beam diameter is about 85 mm, with flat-topped spatial intensity distribution. In the grating compressor, the standard grating groove density and the incident angle are 1480 gr/mm and 51° respectively. For this laser, the degradation of focused intensity with grating groove density error is investigated, as shown in Fig. 4. (i) To achieve 0.9 times the ideal focused intensity, the grating groove density error has to be kept below 0.02 gr/mm. (ii) For 0.7 times the ideal focused intensity, the grating groove density error can be relieved to 0.04 gr/mm. (iii) When the grating groove density error reaches up to 0.2 gr/mm, the attainable focused intensity is only ~ 10% of the ideal focused intensity. Therefore, a strict control of the groove density mismatching of compression gratings is quite important, even for a 200TW class femtosecond laser.

To compensate the influence of groove density mismatching in double-grating compressors, Zhao and Zuo et al. corrected the angular drift of output laser beam by horizontally rotating the $G2$, i.e., grating tilt[47,48]. By this way, an extra horizontal angular error is introduced, which can cancel out the output beam drift. Nevertheless, this method can only correct the offset angle of central wavelength component, while those of other wavelength components still exist. More importantly, the residual angular chirp of the output laser beam will become more complex. Because the angular chirp induced by grating tilt depends on wavelength, whereas that resulted from grating groove density mismatching does not.

Assuming that the grating groove density error of the compressor in above 200TW laser is 0.1 gr/mm, we calculate the residual offset angle and angular chirp across the full spectrum after correcting the offset angle of the central wavelength. The results are presented in Fig. 5. As shown in Fig. 5a, although the offset angle of the center wavelength is zero, it will increase with the deviation of wavelength to both sides. The beam divergence angle across the full spectrum exceeds 40 μrad. Consequently, the residual angular chirp changes from a constant (0.32 μrad/nm) to wavelength dependent variables, and the residual angular chirp is becoming larger (from the red line to blue line in Fig. 5b). It means that the laser focused intensity degradation will be more significant after employing above compensation method. Therefore, a more efficient compensation scheme is necessary and of great importance.

Here, a new compensation scheme is proposed to control the impacts of groove density mismatching in double-grating compressors. This method also introduces an extra horizontal angular error by grating tilt, but is based on the compensation of angular chirp (rather than offset angle) of the output laser. When $G2$ is tilted
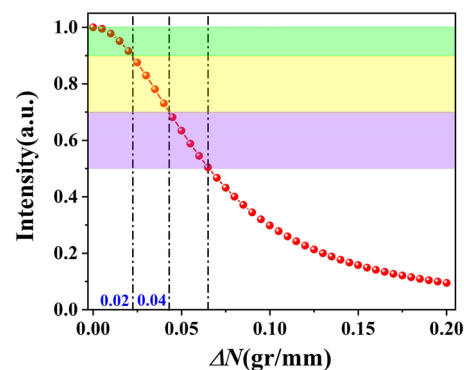

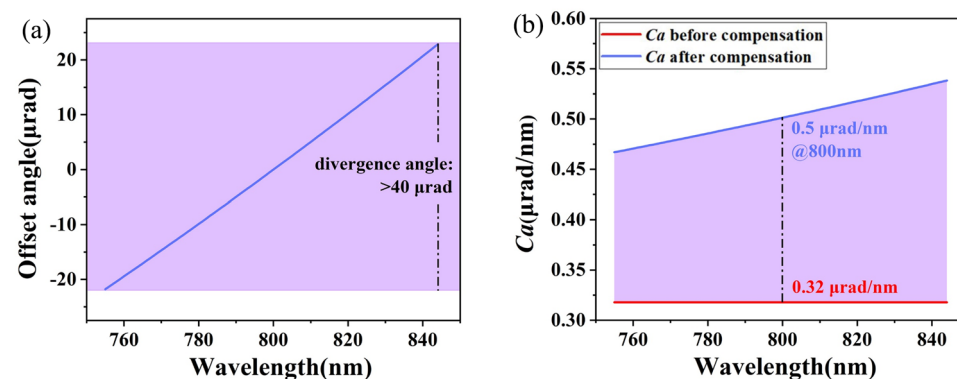**Figure 4.** Variations of focused intensity of the 200TW laser with groove density error.

Figure 5. The effects of compensating for the offset angle of the central wavelength. (**a**) The residual offset angles of different wavelength. (**b**) The residual angular chirp across the spectrum before and after compensation.

from the parallel position by an angle ε_x, the resulting horizontal angular chirp can be expressed as Eq. (6). To compensate the angular chirp, the sum of Eqs. (2) and (6) should be zero. As a result, the tilted angle ε_x of $G2$ is illustrated as Eq. (7). Due to the ε_x is wavelength dependent, the value corresponding to the center wavelength can be further expressed as Eq. (8).

$$C_{ax} = 2\varepsilon_x N \frac{tan\beta}{cos\alpha} \qquad (6)$$

$$\varepsilon_x = \frac{N - N\prime}{N \cdot tan\beta} \qquad (7)$$

$$\varepsilon_{x0} = \frac{N - N\prime}{N \cdot tan\beta_0} \qquad (8)$$

The residual offset angle and angular chirp of output laser after correcting the angular chirp of central wavelength are also calculated and shown in Fig. 6. As shown in Fig. 6a, the offset angle of output laser increases across the full spectrum, but the beam divergence angle is greatly decreased, with a maximum value of ~ 1.5 μrad. Accordingly, the residual angular chirp is also reduced (from the red line to blue line in Fig. 6b). The residual angular chirps at two sides of the spectrum are about ± 0.06 μrad/nm. It is clearly that both the beam divergence and residual angular chirp are better controlled by this new compensation scheme. In the following work, the absolute value of the maximum residual angular chirp is adopted to represent the angular chirp across full spectrum, for the sake of simplicity.

Based on the angular chirp compensation scheme, the variation of effective pulse duration and focused intensity before and after compensation are also compared, as Fig. 7a shows. In the case of a groove density error of 0.2 gr/mm, the broadening factor of effective pulse duration is reduced from 4 to 1.2 and the focused intensity is increased from 10% to 72% of the ideal value, after the compensation. The simulated results demonstrate the effectiveness of our compensation scheme.
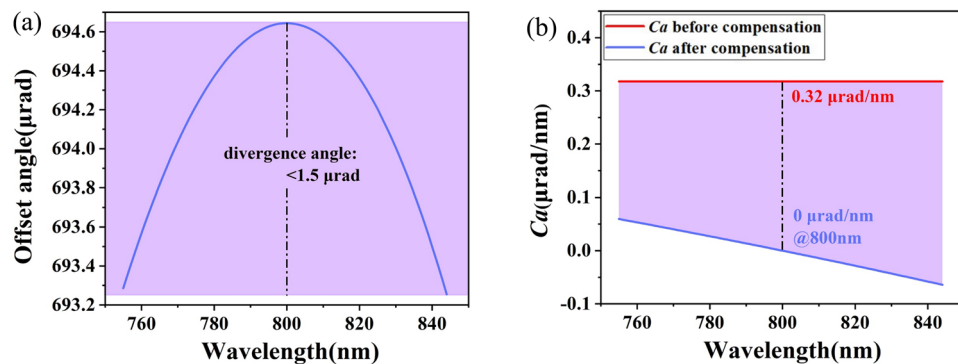

Figure 6. The effects of compensating for the angular chirp of the central wavelength. (**a**) The residual offset angles of different wavelength. (**b**) The residual angular chirp across the spectrum before and after compensation.
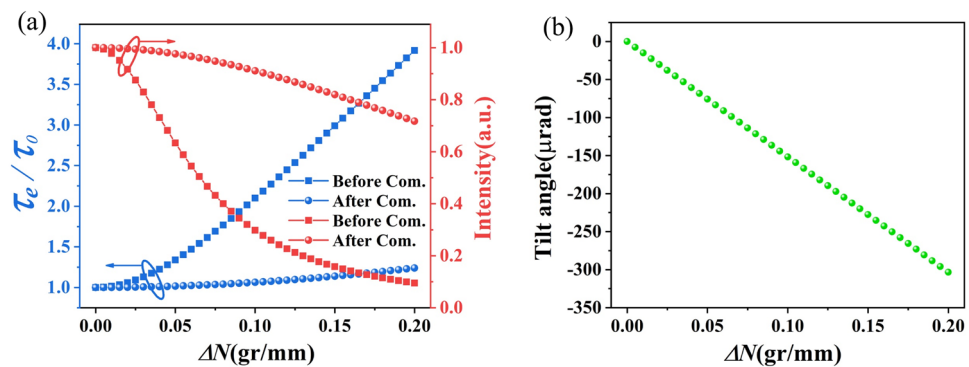

Figure 7. (**a**) Focused intensity and effective pulse duration broadening factor before and after compensation for angular chirp (Com.: Compensation). (**b**) Corresponding grating tilt angles.

Besides, the required grating tilted angles to compensate different groove density errors are also calculated and shown in Fig. 7b. With the grating groove density error increases from zero to 0.2 gr/mm, the grating tilted angle has to linearly increase from zero to − 320 μrad. The negative sign means that the grating $G2$ needs to be clockwise rotated for angular chirp compensation. Generally, the grating groove density error should be better than 0.05 gr/mm, it corresponds to a grating tilt angle below 75 μrad which is too small to obviously affect the compressed pulse duration.

The compensation scheme for four-grating compressors

For PW and higher peak power femtosecond lasers, their beam apertures have to be very large (hundreds of millimeters) in order to avoid optical damage. Hence, four-grating compressors are generally equipped. In addition, the spectra of such ultra-intense lasers are usually very broad to achieve a shorter pulse duration. As a result, the spatiotemporal aberrations induced by the grating groove density mismatching can be more serious. Thereby, the investigation of the groove density mismatching of compression gratings for ultra-intense femtosecond lasers is particularly important. In this section, three ultra-intense femtosecond lasers will be studied for examples. Two of them are CPA-based 1PW and 10PW lasers[6,11], another is OPCPA-based 100PW laser under construction[17].

For simplicity, the beams of above three lasers are assumed to be circular with Gaussian spectra profile. Then the schematic of grating groove density mismatching in four-grating compressors can be illustrated as Fig. 2. The detailed parameters of above three ultra-intense femtosecond lasers are described in Table 1.

Based on these parameters, the focused intensity degradations with the groove density error of compression gratings are calculated, as shown in Fig. 8. It is clear that the focused intensity is rapidly dropping with the grating groove density error increases. And the rate of degradation increases with the increase of laser peak power, because a higher peak power generally indicates a broader spectrum and a larger beam size. From the figure, the mismatching tolerances of these three lasers can be obtained when the focused intensities are 85%, 70% and 50% of the ideal values. We can find that the currently detectable grating groove density error (0.005 gr/mm) is small enough for PW-level lasers, only resulting in ~ 3% focused intensity degradation. Therefore, the grating groove density mismatching is not a big issue for the widely used PW-level lasers. However, when the laser peak power reaches up to 10PW and 100PW, such an error will result in ~ 20% and ~ 80% focused intensity degradation, respectively. Therefore, it is a considerable challenge for the manufacture and test of large-size gratings in 100PW-level lasers. As an error small to 0.005 gr/mm can cause obvious destruction to the focused intensity of 10PW-level and 100PW-level lasers, it is very important to find solutions to suppress the impacts of groove density mismatching in four-grating compressors.

In order to control the angular chirp induced by the grating groove density mismatching of four-grating compressors, a two-step compensation method is proposed. Based on Eq. (4), it is obvious that the angular chirp is decided by ΔN_f. Hence, the first compensation step is to optimize the arrangement of four gratings to make ΔN_f as small as possible, which minimizes angular chirp in the case of parallel grating pairs. The second compensation step is to tilt the $G4$ for introducing a horizontal angular error to further compensate the residual angular chirp, which is similar to the new scheme proposed in Section "A new compensation scheme for double-grating compressors". The optimal tilt angle of $G4$ corresponding to the central wavelength can be expressed as Eq. (9). If ε_x is positive, the grating tilts clockwise; Otherwise, it tilts counterclockwise.

Peak power (PW)	Beam aperture (mm)	Bandwidth (nm)	Center wavelength (nm)	Incident angle	Groove density (gr/mm)	Duration (fs)
1	213.5	80	800	51°	1480	29.6
10	470	100	800	51.5°	1480	21
100	830	210	925	61°	1400	15

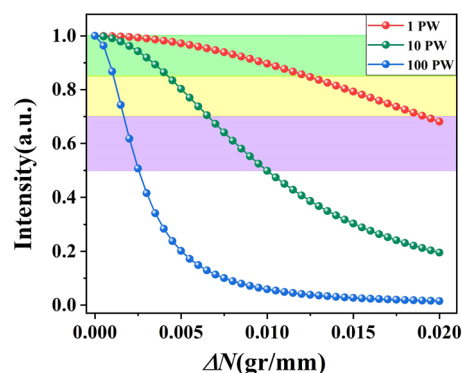**Table 1.** Laser parameters and grating configurations with different peak powers.

Figure 8. Focused intensity deterioration with grating groove density errors for 1PW, 10PW and 100PW lasers.

$$\varepsilon_{x0} = \frac{(N2+N3)-(N1+N4)}{tan\gamma_0 \cdot (N2+N3-N1)} \tag{9}$$

Besides, a relatively simple case is investigated for example, in which the four-grating compressor happens to be the mirror-symmetry configuration of a double-grating compressor (i.e., N–N'–N'–N). Two optimization schemes are proposed for the arrangement of four gratings.

Firstly, the positions of G3 and G4 are switched. The order of grating groove density changes to N–N'–N–N', as Fig. 9a shows. In this case, for the aforementioned 100PW laser, when the groove density mismatching does not exceed 0.5 gr/mm, the angular chirp introduced by the first grating pair (G1 and G2) will be completely compensated by the second grating pair (G3 and G4), based on the grating diffraction equation. The current grating manufacturing and testing technology is easy to control such an amount of mismatching (0.5 gr/mm), indicating that our method is effective. However, due to the groove density mismatching, a small spatial chirp will be lastly introduced to the edges of the output laser beam. When N'>N, the short- and long-wavelength components will at the upper and lower edges of the output laser beam respectively, as shown in Fig. 9a. While N'<N, the exact opposite happens. In addition, groove density mismatching between G1 and G2 is the causation for the final asymmetric spatial chirp. For the 100PW laser, the spatial chirp widths D_1 and D_2 are 0.4 mm and 0.3 mm respectively, assuming the grating groove density error is as large as 0.1 gr/mm. Such spatial chirp width is negligible with respect to the beam size (830 mm), for the total spatial chirp width only accounts for 0.08% of the beam size. Compared with other works which have tens of millimeters spatial chirp width[49,50], spatial chirp in our work can hardly affect the spatiotemporal characteristics of laser pulses.

Secondly, the positions of G2 and G4 are exchanged. The order of grating groove density becomes N–N–N'–N', as shown in Fig. 9b. Under this situation, the groove densities in each grating pair are matched, and hence no angular chirp is introduced. Similar to Fig. 9a, due to the groove density mismatching, traces of spatial chirp will be lastly introduced to the edges of the output laser beam. For the aforementioned 100PW laser, the distribution of spatial chirp is symmetric and the total spatial chirp widths ($D_1 + D_2$) of the output laser beams is only 0.1 mm, when the grating groove density error is as large as 0.1 gr/mm. With respect to the beam size (830 mm), the total spatial chirp width only accounts for 0.01% of the beam size. Besides, the residual spatial chirp can also be eliminated by slightly changing the separation between G3 and G4. Therefore, compared with exchanging the positions of G3 and G4, exchanging the positions of G2 and G4 can more effectively eliminate the impact of grating groove density mismatching in four-grating compressors.

In short, a two-step compensation method is proposed to control the angular chirp in four-grating compressors. Particularly, when the four-grating compressor happens to be the mirror-symmetry configuration of a double-grating compressor, the angular chirp can be completely eliminated just by optimizing the arrangement of four gratings.

Conclusion

In conclusion, we investigate the angular chirp and the resulting spatiotemporal aberrations induced by the groove density mismatching of compression gratings in this work. The results show that the degradation of effective focused intensity induced by grating groove density mismatching will aggravate with the increase of spectral bandwidth or beam aperture. For the 100PW-level laser, even the groove density error as small as 0.001 gr/mm can cause a 15% drop of effective focused intensity. Therefore, it is of crucial importance to find solutions to overcome the impact of the grating groove density mismatching. For the double-grating compressors, a new compensation scheme based on the suppression of the angular chirp, rather than the offset angle of output laser beam is proposed and demonstrated. Meanwhile, groove density mismatching in four-grating compress can be
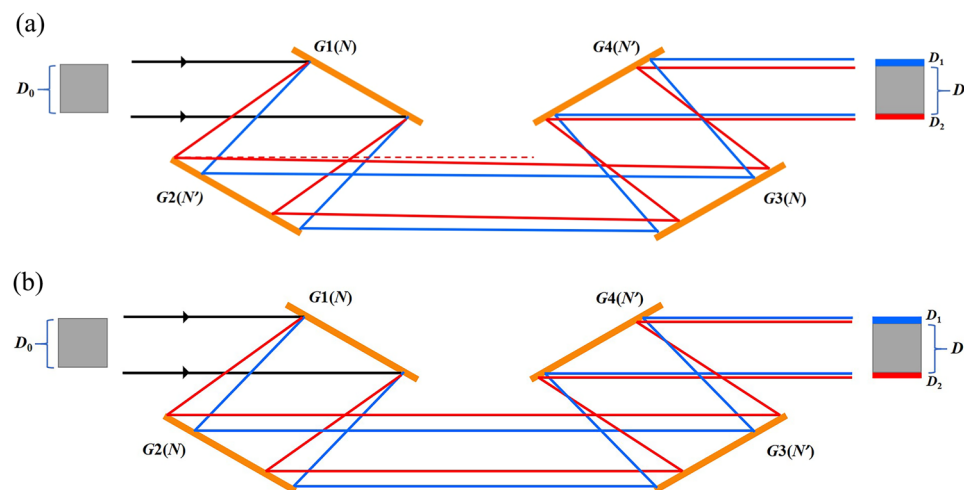

Figure 9. Compensation for grating groove density mismatching by (**a**) switching G3 and G4, (**b**) exchanging G2 and G4.

compensated by a two-step compensation method. This work indicates the importance of groove density matching of compression gratings, and offer helpful guidelines for the design of the ultra-intense femtosecond lasers.

Data availability

References

1. Strickland, D. & Mourou, G. Compression of amplified chirped optical pulses. *Opt. Commun.* **55**, 447–449 (1985).
2. Dubietis, A., Jonusauskas, G. & Piskarskas, A. Powerful femtosecond pulse generation by chirped and stretched pulse parametric amplification in BBO crystal. *Opt. Commun.* **88**, 437–440 (1992).
3. Xu, Y. *et al.* A Stable 200TW/1Hz Ti:sapphire laser for driving full coherent XFEL. *Opt. Laser Technol.* **79**, 141–145 (2016).
4. Wu, F. *et al.* Performance improvement of a 200TW/1Hz Ti:sapphire laser for laser wakefield electron accelerator. *Opt. Laser Technol.* **131**, 106453 (2020).
5. Aoyama, M. *et al.* 0.85-PW, 33-fs Ti: Sapphire laser. *Opt. Lett.* **28**, 1594–1596 (2003).
6. Zhang, Z. *et al.* The 1 PW/01 Hz laser beamline in SULF facility. *High Power Laser Sci. Eng.* **8**, e4 (2020).
7. Yu, T. J. *et al.* Generation of high-contrast, 30 fs, 1.5 PW laser pulses from chirped-pulse amplification Ti:sapphire laser. *Opt. Express* **20**, 10807–10815 (2012).
8. Zeng, X. *et al.* Multi-petawatt laser facility fully based on optical parametric chirped-pulse amplification. *Opt. Lett.* **42**, 2014–2017 (2017).
9. Bahk, S. W. *et al.* Generation and characterization of the highest laser intensities (10^{22} W/cm^2). *Opt. Lett.* **29**, 2837–2839 (2004).
10. Yoon, J. W. *et al.* Realization of laser intensity over 10^{23} W/cm^2. *Optica* **8**, 630–635 (2021).
11. Li, W. *et al.* 339 J high-energy Ti:sapphire chirped-pulse amplification for 10 PW laser facility. *Opt. Lett.* **43**, 5681–5684 (2018).
12. Radier, C. *et al.* 10 PW peak power femtosecond laser pulses at ELI-NP. *High Power Laser Sci. Eng.* **10**, e21 (2022).
13. Batysta, F. *et al.* Spectral pulse shaping of a 5 Hz, multi-joule, broadband optical parametric chirped pulse amplification frontend for a 10 PW laser system. *Opt. Lett.* **43**, 3866–3869 (2018).
14. Cimmino, A. *et al.* Radiation protection at Petawatt laser-driven accelerator facilities: The ELI beamlines case. *Nucl. Sci. Eng.* **198**, 245–263 (2024).
15. Bromage, J. *et al.* MTW-OPAL: A technology development platform for ultra-intense optical parametric chirped-pulse amplification systems. *High Power Laser Sci. Eng.* **9**, e63 (2021).
16. Hu, J. *et al.* Numerical analysis of the DKDP-based high-energy optical parametric chirped pulse amplifier for a 100 PW class laser. *Appl. Opt.* **60**, 3842–3848 (2021).
17. Wu, F. *et al.* Dispersion management for a 100 PW level laser using a mismatched-grating compressor. *High Power Laser Sci. Eng.* **10**, 1–12 (2022).
18. Mukhin, I. B. *et al.* Design of the front-end system for a subexawatt laser of the XCELS facility. *Quantum Electron.* **51**, 759–767 (2021).
19. Cartlidge, E. Eastern Europe's laser centers will debut without a star. *Science* **355**, 785–785 (2017).
20. Gabolde, P., Lee, D., Akturk, S. & Trebino, R. Describing first-order spatio-temporal distortions in ultrashort pulses using normalized parameters. *Opt. Express* **15**, 242–251 (2007).
21. Li, Z. *et al.* Fourth-order dispersion compensation for ultra-high power femtosecond lasers. *Opt. Commun.* **357**, 71–77 (2015).
22. Wu, F. *et al.* A novel design of double chirped pulse amplification laser systems for fourth-order dispersion control. *Opt. Express* **28**, 31743–31753 (2020).
23. Fiorini, C. *et al.* Temporal aberrations due to misalignments of a stretcher-compressor system and compensation. *IEEE J. Quantum Electron.* **30**, 1662–1670 (1994).
24. Pretzler, G., Kasper, A. & Witte, K. J. Angular chirp and tilted light pulses in CPA lasers. *Appl. Phys. B* **70**, 1–9 (2000).
25. Osvay, K. *et al.* Angular dispersion and temporal change of femtosecond pulses from misaligned pulse compressors. *IEEE J. Sel. Top. Quantum Electron.* **10**, 213–220 (2004).
26. Li, Z., Leng, Y. & Li, R. Further development of the short-pulse Petawatt laser: Trends, technologies, and bottlenecks. *Laser Photonics Rev.* **17**, 2100705 (2023).
27. Li, Z., Tsubakimoto, K., Yoshida, H., Nakata, Y. & Miyanaga, N. Degradation of femtosecond petawatt laser beams: Spatio-temporal/spectral coupling induced by wavefront errors of compression gratings. *Appl. Phys. Express* **10**, 2702 (2017).
28. Li, Z. & Miyanaga, N. Simulating ultra-intense femtosecond lasers in the 3-dimensional space-time domain. *Opt. Express* **26**, 8453–8469 (2018).
29. Leroux, V., Eichner, T. & Maier, A. R. Description of spatio-temporal couplings from heat-induced compressor grating deformation. *Opt. Express* **28**, 8257–8265 (2020).
30. Liu, F. *et al.* Compression grating alignment by far-field monitoring. *Appl. Phys. B* **101**, 587–591 (2010).
31. Boedefeld, R., Hornung, M., Hein, J. & Kaluza, M. C. High precision elimination of angular chirp in CPA laser systems with large stretching factors or high bandwidth. *Appl. Phys. B* **115**, 419–426 (2014).
32. Zhao, Y. *et al.* Investigation of compression grating misalignment in ultra-high peak power femtosecond laser systems. *Appl. Phys. B* **129**, 53 (2023).
33. Misumi, I., Gonda, S., Sato, O., Huang, Q. & Kurosawa, T. Nanometric lateral scales as CRM candidates for AFM, SEM and optical diffractometer. In *7th Symposium on Measurement Technology and Intelligent Instruments, Journal of Physics Conference Series* 206–215 (2005).
34. Chernoff, D. A., Buhr, E., Burkhead, D. L. & Diener, A. Picometer-scale accuracy in pitch metrology by optical diffraction and atomic force microscopy. In *Conference on Metrology, Inspection, and Process Control for Microlithography XXII.* Proceedings of SPIE (2008).
35. Cocco, D., Sostero, G. & Zangrando, M. Technique for measuring the groove density of diffraction gratings using the long trace profiler. *Rev. Sci. Instrum.* **74**, 3544–3548 (2003).
36. Lim, J. & Rah, S. Technique for measuring the groove density of a diffraction grating with elimination of the eccentricity effect. *Rev. Sci. Instrum.* **75**, 780–782 (2004).
37. Liu, B., Wang, Q. P., Xu, X. D. & Fu, S. J. Measurements of groove density for concave gratings with the long trace profiler. *Rev. Sci. Instrum.* **77**, 046106 (2006).
38. Yoon, T. H., Il Eom, C., Chung, M. S. & Kong, H. J. Diffractometric methods for absolute measurement of diffraction-grating spacings. *Opt. Lett.* **24**, 107–109 (1999).

39. Du, L., Du, X. & Wang, Q. Two-dimensional groove density measurement for gratings by diffraction method. In *12th International Conference on Synchrotron Radiation Instrumentation (SRI)*. AIP Conference Proceedings (2015).
40. Sheng, B., Chen, G., Huang, Y. & Luo, L. Measurement of grating groove density using multiple diffraction orders and one standard wavelength. *Appl. Opt.* **57**, 2514–2518 (2018).
41. Guo, C. & Zeng, L. Measurement of period difference in grating pair based on compensation analysis of phase difference between diffraction beams. *Appl. Opt.* **48**, 1651–1657 (2009).
42. Photia, T. *et al.* High-precision grating period measurement. *Appl. Opt.* **58**, 270–273 (2019).
43. Sharma, A. K. & Joshi, A. S. On the estimation of absolute grating groove density and inter-grating groove density errors of laser pulse compression gratings. *Sadhana* **44**, 59 (2019).
44. Kessler, T. J., Bunkenburg, J., Huang, H., Kozlov, A. & Meyerhofer, D. D. Demonstration of coherent addition of multiple gratings for high-energy chirped-pulse-amplified lasers. *Opt. Lett.* **29**, 635–637 (2004).
45. Webb, B., Guardalben, M. J., Dorrer, C., Bucht, S. & Bromage, J. Simulation of grating compressor misalignment tolerances and mitigation strategies for chirped-pulse-amplification systems of varying bandwidths and beam sizes. *Appl. Opt.* **58**, 234–243 (2019).
46. Li, Z. & Kawanaka, J. Complex spatiotemporal coupling distortion pre-compensation with double-compressors for an ultra-intense femtosecond laser. *Opt. Express* **27**, 25172–25186 (2019).
47. Zhao, D. *et al.* Effect of grating groove density error on the output pulses of the tiled grating compressor and corresponding compensation scheme. *Acta Phys. Sin.* **66**, 024201 (2017).
48. Zuo, Y. *et al.* Theory of array-grating compressor based on in-pair compensation of errors. *Acta Phys. Sin.* **56**, 5227–5232 (2007).
49. Liu, J., Shen, X., Du, S. & Li, R. Multistep pulse compressor for 10s to 100s PW lasers. *Opt. Express* **29**, 17140–17158 (2021).
50. Du, S. *et al.* A 100-PW compressor based on single-pass single-grating pair. *High Power Laser Sci. Eng.* **11**, e4 (2023).

Author contributions

Funding

Competing interests

The authors declare no competing interests.

Additional information

Correspondence and requests for materials should be addressed to Y.X., Y.L. or R.L.

Reprints and permissions information is available at www.nature.com/reprints.

Publisher's note Springer Nature remains neutral with regard to jurisdictional claims in published maps and institutional affiliations.